

August 1985

LRP 258/85

**POLOIDAL ASYMMETRY OF THE DENSITY PROFILE
ASSOCIATED WITH A FLOW IN A TOKAMAK**

S. Semenzato, R. Gruber, R. Iacono, F. Troyon
and H.P. Zehrfeld

submitted to Physics of Fluids

POLOIDAL ASYMMETRY OF THE DENSITY PROFILE ASSOCIATED WITH
A FLOW IN A TOKAMAK

S. Semenzato, R. Gruber, R. Iacono, F. Troyon and H.P. Zehrfeld*

Centre de Recherches en Physique des Plasmas
Association EURATOM - Confédération Suisse
Ecole Polytechnique Fédérale de Lausanne
21, Av. des Bains, CH-1007 Lausanne/Switzerland

* Max-Planck-Institut für Plasmaphysik, Garching (RFA)

ABSTRACT

In stationary Tokamak equilibria with poloidal and toroidal flows the density is no longer constant on a flux surface. The relationship between the size of the density variation and the direction and magnitude of the flow is examined. The case of a poloidal flow with no net toroidal velocity leads to a large density variation at moderate values of the Mach number. We show as an example that the reported anomalies in the density profiles measured in the PDX Tokamak in presence of strong neutral beam heating could be explained with many different flow patterns.

I. INTRODUCTION

The large amount of neutral beam injection power now available on many Tokamaks has introduced a new dimension in Tokamak physics. Depending on the mode of operation, it should be possible to set the plasma in motion, thus transforming the static Tokamak equilibrium into a steady flow. This possibility has always been recognized either as a dangerous side effect to guard against by keeping, if needed, the injection balanced or as a new degree of freedom which might be used to reach improved performances. But the few attempts at measuring this rotation spectroscopically through the Doppler shift of impurity lines have not revealed velocities as large as could have been expected from simple momentum transfer from the beams¹ and flow has been neglected in the equilibrium reconstruction done from magnetic measurements in, to our knowledge, all cases. Yet this might have been a non-negligible effect in the β limit experiments² so that we have become interested in evaluating quantitatively the effect of a rotation on the equilibrium.

A strong stimulation to this study has come from measurements made on PDX (Princeton Divertor Experiment) which have revealed anomalies in the density and electron temperature profiles whenever the neutral beam injection power was large.³ This experiment utilised a unique diagnostic which provided at a given time in one discharge the full density and electron temperature across the mid-plane with very high resolution (56 channels). The profiles, being like snapshots, give an instantaneous state and do not average fluctuations. This is probably the reason of the remarkable fine structure seen on these profiles. But forgetting these fluctuations, they reveal also that the

density and temperature cannot both be magnetic flux functions. The density profile is strongly asymmetric. In the ohmic regime, there is already an effect but, because of the fluctuations, it might be waved away by arguing on the error bars.

The object of this paper is to study the effect of a stationary flow in a Tokamak on the equilibrium, specially on the density profiles. We use the documented PDX measurements as an example to visualize and quantify these effects.

The plan of the paper is the following. We give a short summary of the basic equations, followed by an analytic evaluation of the effects to be expected. We then solve numerically the equations in a specific configuration with different assumptions on the relative importance of the poloidal and toroidal flows. The implications are then briefly discussed.

II. THE EQUATIONS

Let us introduce the cylindrical coordinate system r, ϕ, z centered on the main axis of the torus and designate by $\psi(r, z)$ the usual magnetic flux function. The plasma is described by the ideal one fluid model with scalar pressure and the flow is assumed to be adiabatic. The isothermal case obtains by replacing $\gamma = 1$.

Let us briefly summarize the equations which describe a stationary flow equilibrium. The details are given in Semenzato et al.^{4,5}.

There are 5 arbitrary functions of ψ which must be specified to define the equilibrium. They are called Φ_E , ψ_M , T_M , C and H . Calling ρ , p , v_p , v_ϕ , B_p , B_ϕ the density, pressure, poloidal and toroidal components of the flow velocity, poloidal and toroidal components of the magnetic field respectively, we have the relations

$$B_p = \frac{|\nabla\psi|}{r}, \quad rB_\phi \equiv T(r, z) = (T_M - r^2 \frac{d\psi_M}{d\psi} \frac{d\Phi_E}{d\psi})/D, \quad (1)$$

$$\rho v_p = B_p \frac{d\psi_M}{d\psi}, \quad (2)$$

$$\rho v_\phi = B_\phi \frac{d\psi_M}{d\psi} - \rho r \frac{d\Phi_E}{d\psi} \quad (3)$$

$$p = C\rho^\gamma \quad (4)$$

$$H = \frac{1}{2} B^2 \left(\frac{d\psi_M}{d\psi}\right)^2 / \rho^2 - \frac{1}{2} r^2 \left(\frac{d\Phi_E}{d\psi}\right)^2 + \frac{\gamma C}{\gamma-1} \rho^{\gamma-1} \quad (5)$$

with the definitions $B^2 \equiv B_\phi^2 + B_p^2$ and $D \equiv 1 - (d\psi_M/d\psi)^2/\rho$. When $\gamma = 1$, the last term in H , $\gamma C \rho^{\gamma-1}/(\gamma-1)$ must be replaced by $C \ln \rho$.

These relations determine all the physical quantities in terms of $\psi(r, z)$ and of the five arbitrary functions of ψ . In particular, the dependence on poloidal angle of all the quantities is given by these relations.

The flux function $\phi(r,z)$ is obtained from the analogue to the Grad-Schlüter-Shafranov (GSS) equation for a static equilibrium

$$\begin{aligned} \underline{\nabla} \cdot \left[D \frac{\underline{\nabla} \phi}{r^2} \right] = & - \frac{T}{r^2} \frac{dT_M}{d\phi} - \rho \frac{dH}{d\phi} + \frac{\rho \gamma}{\gamma-1} \frac{dC}{d\phi} - \frac{1}{\rho} \frac{d^2 \phi_M}{d\phi^2} \left(B^2 \frac{d\phi_M}{d\phi} - \rho T \frac{d\Phi_E}{d\phi} \right) \\ & + \frac{d^2 \Phi_E}{d\phi^2} \left(T \frac{d\phi_M}{d\phi} - \rho r^2 \frac{d\Phi_E}{d\phi} \right) \end{aligned} \quad (6)$$

In case $\gamma = 1$, the term $\rho^\gamma/\gamma-1$ becomes $\rho \ln \rho$. This system of equations can be solved with a finite element code, CLIO, described by Semenzato et al.^{4,5} The plasma surface is assumed to be given and, to guarantee that this surface is simultaneously an isobar and a magnetic surface, we require that the flow velocity vanishes there. Before solving the full system, we can draw some general results concerning the density variation on a magnetic surface just by using the first five equations assuming the magnetic topology is known.

III. POLOIDAL ASYMMETRY DUE TO ROTATION

The rotation velocity is determined by the two quantities $\Phi_E(\psi)$, which is the electrostatic potential, and $\phi_M(\psi)$, the flux of the poloidal momentum. The flow can be decomposed into a flow parallel to the magnetic field \underline{v}_\parallel and a perpendicular flow induced by the electrostatic field, \underline{v}_\perp .

$$\underline{v}_\perp = \frac{B}{\rho} \frac{T}{B^2} \frac{d\Phi_E}{d\psi}, \quad \underline{v}_\perp \cdot \underline{\phi} = - \frac{d\Phi_E}{d\psi} \frac{r B^2}{B^2} \quad (7)$$

$$v_{\parallel p} = B \left(-\frac{1}{\rho} \frac{d\psi_M}{d\psi} - \frac{T}{B^2} \frac{d\Phi_E}{d\psi} \right), \quad v_{\parallel \phi} = \frac{T}{r} \left(-\frac{1}{\rho} \frac{d\psi_M}{d\psi} - \frac{T}{B^2} \frac{d\Phi_E}{d\psi} \right) \quad (8)$$

By choosing $\psi_M \equiv 0$, one can have a pure toroidal rotation resulting from the superposition of a flow parallel to \underline{B} and of a perpendicular flow driven by the electrostatic potential. Choosing instead $\Phi_E = 0$ gives a pure parallel flow. It is interesting to note that it is impossible to have a pure poloidal or perpendicular flow, because of the different poloidal dependences of the coefficients of $d\psi_M/d\psi$ and $d\Phi_E/d\psi$ in Eqs. (3) and (8).

We are particularly interested in the poloidal variation of the density on a magnetic surface. It is found by solving Eq. (5).

In the special case of a purely toroidal flow, $\psi_M \equiv 0$, this dependence is explicit

$$\rho(r, \psi) = \left\{ \frac{\gamma-1}{\gamma C} \left[H + \frac{1}{2} r^2 \left(\frac{d\Phi_E}{d\psi} \right)^2 \right] \right\}^{\frac{1}{\gamma-1}} \quad \text{for } \gamma \neq 1$$

(9)

$$\rho(r, \psi) = \exp \left\{ \frac{H}{C} + \frac{r^2}{2C} \left(\frac{d\Phi_E}{d\psi} \right)^2 \right\} \quad \text{for } \gamma = 1$$

Designating with a bar the values at the major radius R , taken to be the geometric center of the ψ surface, we can rewrite Eq. (9) as

$$\rho = \bar{\rho} \left[1 + \frac{\gamma-1}{2} \frac{r^2-R^2}{c_s^2} \left(\frac{d\Phi_E}{d\psi} \right)^2 \right]^{\frac{1}{\gamma-1}}, \quad \gamma \neq 1 \quad (10)$$

$$\rho = \bar{\rho} \exp\left[\frac{(r^2-R^2)}{2c_s^2} \left(\frac{d\Phi_E}{d\psi} \right)^2 \right], \quad \gamma = 1$$

where $c_s \equiv \sqrt{\gamma \bar{p}/\bar{\rho}}$ is the average sound velocity. Note that $R^2(d\Phi_E/d\psi)^2 = \bar{v}_\phi^2$ so that the term which gives the poloidal dependence of the density can be rewritten as $(r^2-R^2)(\bar{v}_\phi^2/c_s^2)$, which shows that the effect of flow scales with the sound speed and will only be visible at flow velocities approaching the sound velocity.

For $\bar{v}_\phi/c_s \ll 1$, the two relations (10) give the leading dependence

$$\rho \approx \bar{\rho} \left(1 + \frac{r^2-R^2}{2R^2} \frac{\bar{v}_\phi^2}{c_s^2} \right) \quad (11)$$

Flow always leads to an asymmetry of the density profile corresponding to an outward shift.

The other special case of a purely parallel flow with $\Phi_E \equiv 0$ can be treated in the same way except that ρ comes in nonlinearly in

the equations. For $\left| \frac{(r-R)}{R} \frac{v_\phi}{c_s} \right| \ll 1$ and $\Delta \left(\frac{v_\phi^2}{c_s^2} \right) \ll 1 - \frac{v_\phi^2}{c_s^2}$, where Δ

designates the maximum variation on the given magnetic surface, the density can be approximated by

$$\rho \approx \bar{\rho} \left\{ 1 - \frac{\frac{B^2 - \bar{B}^2}{2\bar{\rho}^2 c_s^2} \left(\frac{d\psi_M}{d\psi}\right)^2}{1 - \frac{\bar{B}^2}{\bar{\rho}^2 c_s^2} \left(\frac{d\psi_M}{d\psi}\right)^2} \right\} \approx \bar{\rho} \left\{ 1 - \frac{\frac{B^2 - \bar{B}^2}{2\bar{B}^2} \frac{\bar{v}_\phi^2}{c_s^2}}{1 - \frac{\bar{B}^2}{\bar{\rho}^2 c_s^2} \left(\frac{d\psi_M}{d\psi}\right)^2} \right\} \quad (12)$$

The density is again asymmetric with an outward shift since B decreases as r increases. In the leading order $B_p^2 \ll B^2$, $\beta_p \sim 1$, the formula (12) reduces to

$$\rho = \bar{\rho} \left(1 + \frac{\bar{v}_\phi^2 / c_s^2}{1 - \bar{v}_\phi^2 / c_s^2} \frac{r - R}{R} \right), \quad (13)$$

From these two examples one might conclude that it is always necessary to have a \bar{v}_ϕ in the range of c_s to have a measurable effect on the density profile. This is not correct as we now show.

Expanding the various terms of (5) around the mid-point R , the density can be approximated by ^{6,7}

$$\rho \approx \bar{\rho} \left\{ 1 - \frac{\frac{B^2 - \bar{B}^2}{2\bar{\rho}^2 c_s^2} \left(\frac{d\psi_M}{d\psi}\right)^2 - \frac{r^2 - R^2}{2c_s^2} \left(\frac{d\psi_E}{d\psi}\right)^2}{1 - \frac{\bar{B}^2}{\bar{\rho}^2 c_s^2} \left(\frac{d\psi_M}{d\psi}\right)^2} \right\} \quad (14)$$

The effects of $d\psi_M/d\psi$ and $d\psi_E/d\psi$ are additive on the density variation.

The parallel flow velocity can be also expanded around the mid-point R:

$$v_{\parallel} \approx \frac{\bar{B}}{\bar{\rho}} \frac{d\psi_M}{d\psi} - R \frac{d\Phi_E}{d\psi} + \frac{\frac{B-\bar{B}}{\bar{\rho}} \frac{d\psi_M}{d\psi} - (r-R) \frac{d\Phi_E}{d\psi}}{1 - \frac{B^2}{\rho^2 c_s^2} \left(\frac{d\psi_M}{d\psi}\right)^2} \quad (15)$$

The effect of the two terms $d\psi_M/d\psi$ and $d\Phi_E/d\psi$ can be either additive or subtractive. By choosing

$$\frac{\bar{B}}{\bar{\rho}} \frac{d\psi_M}{d\psi} = R \frac{d\Phi_E}{d\psi} = \bar{\rho} \bar{v}_p \quad (16)$$

$\bar{v}_{\parallel} = 0$, and v_{\parallel} reduces to a pure $m = 1$ flow on the surface.

The density variation then becomes

$$\rho = \bar{\rho} \left(1 + 2 \frac{\frac{\bar{v}_p^2 \bar{B}^2}{\bar{B}^2 c_s^2} \frac{p}{s} \frac{r-R}{R}}{1 - \frac{p}{\bar{B}^2 c_s^2}} \right) \quad (17)$$

and the parallel flow velocity

$$v_{\parallel} = 2 \frac{r-R}{R} \frac{\frac{\bar{B}/\bar{B}}{\bar{B}^2 \bar{v}_p^2} \frac{p}{s}}{1 - \frac{p}{\bar{B}^2 c_s^2}} \bar{v}_p \quad (18)$$

which, for large aspect ratio, circular cross-section reduces to

$$v_{\parallel} = 2q \bar{v}_p \cos\theta / \left(1 - q^2 \frac{\bar{v}_p^2 R^2}{c_s^2 \rho_s^2} \right) \quad (19)$$

where q is the safety factor and ρ_s the small radius of the ψ surface considered, θ the poloidal angle.

A convenient way of rewriting the relations (18) and (19) is to express the flow velocities in terms of the density asymmetry A defined as

$$A(\psi) \equiv \frac{\rho - \bar{\rho}}{r - R} \cdot \frac{R}{\bar{\rho}} \quad (20)$$

Then (18) becomes

$$v_{\parallel} = \sqrt{A(A + 2)} \frac{r - R}{R} c_s \quad (21)$$

and (19):

$$\bar{v}_p = \sqrt{\frac{A}{A + 2}} \left(\frac{\rho_s}{Rq} \right) c_s \quad (22)$$

The expansion used to derive (14) is valid provided

$$\frac{\bar{v}_p^2 B^2}{B_p^2 c_s^2} \ll 1 \quad \text{and} \quad \Delta \left(\frac{v^2 B^2}{B_p^2 c_s^2} \right) \ll 1 - \frac{v^2 B^2}{B_p^2 c_s^2} \quad (23)$$

We now look at the experimental evidence we have found out and analyse it with the help of CLIO.

III. NUMERICAL STUDY OF AN EXPERIMENTAL ANOMALY

We have found in the literature a well-documented case which we use as basis for a parametric study.³ It is a high β PDX equilibrium. We know the electron temperature and the electron density profiles in the equatorial plane. We also know the global characteristics of the discharge: major radius $R = 1.43\text{m}$, circular cross-section with minor radius $a = 0.42\text{m}$, $B_\phi = 1.5\text{ T}$, $I = 450\text{ kA}$, safety factor on axis $q_0 \sim 1$, $\beta \sim 2.5\%$ with $\beta_I \sim 1$, $n_{e0} \sim 10^{14}\text{cm}^{-3}$ and $T_{e0} \sim 1.2\text{ keV}$. We do not have information on the ion population, neither on the bulk nor on the beam component which must be sizeable. The high parallel thermal conductivity of the electrons makes it highly plausible that the electron temperature is constant on a magnetic surface.

In a first step, we construct a static scalar pressure equilibrium which satisfies all the global constraints, with a mean temperature profile proportional to the electron temperature profile. It is characterized by the three profiles

$$\begin{aligned} p &= p_0 (1 - 1.604s^2 + 0.211s^4 + .393s^6) \\ T &= T_0 (1 + 0.008s^2 - 0.004s^4) \\ \rho &= \rho_0 (1 - 0.2s^2 - 0.7s^4) \end{aligned} \quad (24)$$

where $s \equiv \sqrt{1-\psi/\psi_0}$, ψ_0 the flux on axis. ψ is normalized to vanish at the boundary. The index o refers to the values on axis. At the edge $\rho = 0.1\rho_0$. Figure 1 shows the comparison of temperature and density with the experimental results. The central $\beta_0 \equiv p_0/(B^2/2)$ is

7.4% while all the global parameters fit the available data. The central mean temperature is 2.1 keV if the electron density on axis is taken to be 10^{14} cm^{-3} ($Z=1$). Since $T_{e0} = 1.2 \text{ keV}$, $T_{i0} = 4.0 \text{ keV}$, which includes the beam contribution. We have no information to check this. The observed density profile is different from the fitted one and it has the characteristic asymmetry expected from the presence of a flow. We try to quantify the flow velocity which is needed to explain by itself this asymmetry in density.

To be able to use CLIO, we have to make some assumptions.⁴ Since it is a scalar pressure code, we must assume that $\gamma = 1$ to enforce that the electron temperature be constant on a flux surface. The code requires $\gamma \neq 1$ so that we set $\gamma = 1.01$. From the static fit there is no evidence that the electron temperature presents the same anomaly as the density. This brings support to the assumption $\gamma \approx 1$.

CLIO does not use as input the five flux functions but instead these functions are calculated from the profiles of T_m , ρ , p , $v_p^* = v_p/rBp$ and v_ϕ on half the equatorial plane, between the inner surface and the magnetic axis, the so-called "reference line". For convenience these profiles are expressed in terms of the same reduced flux s . They are polynomials in s . Because of the shift of the pressure axis with respect to the magnetic axis there must be odd powers of s which can be adjusted to avoid discontinuities in the derivatives of the various physical quantities. Details are given in Semenzato et al.^{4,5} To keep the plasma surface as both an isobar $p = 0$ and a magnetic surface we require that $\underline{v} = 0$ on the surface. We only consider here the results.

Three equally good fits have been obtained with three different flows.

The first one is made by assuming a purely toroidal flow. The source functions on the reference line are ($c_{SO} = \sqrt{\gamma p_O / \rho_O}$)

$$\begin{aligned}
 T &= T_O (1 + 0.0080s^2 - 0.0040s^4) \\
 P &= p_O (1 - 0.199s - 1.475s^2 + 0.450s^4 + 0.224s^6) \\
 \rho &= \rho_O (1 - 0.198s - 0.002s^2 - 0.7s^4) \\
 v_\phi &= c_{SO} (0.921 - 0.215s - 0.706s^2) \\
 v_P &= 0.
 \end{aligned}
 \tag{25}$$

Figures 2(a) and 2(b) show the fitting to the experimental results. The pressure on axis p_O is practically unchanged compared to the static fit. Figures 2(c) and 2(d) present the profiles of T , p and v_ϕ across the plasma in the equatorial plane. The temperature profile is little affected by the rotation. The density profile is reasonably well fitted. The vertical field to maintain the equilibrium is deduced from the poloidal field at the surface. The toroidal flow multiplies the vertical field by 2.1 compared to the static fit. The linear variation of the density in the central region means, according to Eq. 13, that the average density profile is flat and that the Mach number $M = v_\phi / c_S$ is also flat. The value obtained by fitting Eq. (13) to the experimental data is compatible with the value on axis 0.94 in Eq. (23). This is too large according to the spectroscopic measurements of the rotation velocity made on analogous discharges.¹

As seen in the previous section it is possible to obtain the same density variations with a smaller toroidal velocity which has an $m = 1$ poloidal dependence. With the reference line method it is difficult to have strictly no average toroidal flow on each surface. Nevertheless the following choice of source functions

$$\begin{aligned}
 T &= T_0 (1 + 0.0152s - 0.0148s^2 + 0.0036s^4) \\
 p &= p_0 (1 - 0.375s - 1.162s^2 + 0.263s^4 + 0.274s^6) \\
 \rho &= \rho_0 (1 - 0.371s + 0.171s^2 - 0.7s^4) \\
 v_\phi &= c_{s0} (0.566s - 0.566s^2) \\
 v_p^* &\equiv \frac{v_p}{rB_p} = \frac{c_{s0}}{T_0} (0.653 + 0.399s - 1.052s^2)
 \end{aligned} \tag{26}$$

is not far from such a solution. Figure 3 shows the various profiles across the equatorial plane. The values of β_0 and β are essentially unchanged as in the preceding case. The magnetic topology is also unchanged and the vertical field changes only by a few percents. The only measurable change is on the density profile which is very well fitted. The $m = 1$ dependence of v_ϕ is evident and the maximum value is reached off axis. It is $0.23 c_{s0}$. The poloidal velocity shown in Fig. 3(e) is also normalized to c_{s0} and is much smaller (maximum Mach number of 0.06). We have compared analytical and numerical values of the normalized radial gradients of poloidal and parallel plasma velocities and found complete agreement.

These two fits are extreme cases and one can have any intermediate fit. In presence of NBI one might consider the situation where

v_ϕ does not change sign, but is nevertheless minimum, as a more significant limiting case than the last one. The following choice of source functions

$$\begin{aligned}
 T &= T_0 (1 + 0.0096s - 0.0064s^2 + 0.0008s^4) \\
 p &= p_0 (1 - 0.242s - 1.316s^2 + 0.233s^4 + 0.325s^6) \\
 \rho &= \rho_0 (1 - 0.239s + 0.039s^2 - 0.7s^4) \\
 v_\phi &= c_{s0} (-0.151 + 0.413s - 0.262s^2) \\
 v_p^* &\equiv \frac{v_p}{rB_p} = \frac{c_{s0}}{T_0} (0.521 + 0.249s - 0.770s^2)
 \end{aligned} \tag{27}$$

give also a good fit while v_ϕ almost vanishes on the inside of the torus. The resulting profiles are shown in Fig. 4. The maximum of v_ϕ is about $0.3 c_{s0}$.

IV. CONCLUSIONS

From these three fits one can deduce some interesting results which are probably general. A pure toroidal rotation only has an effect if it is near sonic and if it leads to a substantial change in the vertical field in addition to the density asymmetry. The introduction of a small poloidal component can produce the same density asymmetry without changing the magnetic structure and all the other global plasma parameters. These results suggest that it may be easier to find evidence of poloidal plasma rotation by measuring the density across the equatorial plane, together with magnetic measurements, than by

spectroscopic measurements. Spectroscopic measurements should be done in such a way that the full profile of v_ϕ is obtained. Measuring v_p looks very difficult and ineffective since v_ϕ is always much larger.

These conclusions are naturally limited by the validity of the model. It would be desirable to extend the work to handle non-isotropic pressure and multicomponent ion populations to allow for the beam component and to be able to impose different equations of state for electrons and ions.

Acknowledgements

Conversations with Dr. K. McGuire of the PDX team and Dr. C. Daughney, a member of the Princeton diagnostics group which developed and exploited this high resolution laser diagnostics, have convinced us that the anomalies were real and worth investigating because of their general character.

References

- ¹ K. Braun et al., Nucl. Fusion 23, 1643 (1983).
- ² F. Troyon and R. Gruber, Phys. Letters 110A, 29 (1985).
- ³ B. Johnson et al., Plasma Physics and Controlled Nuclear Research, IAEA, Vienna (1982), Vol. 1, p. 9.
- ⁴ S. Semenzato et al., Comp. Physics Reports, 1, 389 (1984).
- ⁵ S. Semenzato et al., Thesis, Ecole Polytechnique Fédérale 1985 de Lausanne.
- ⁶ H.P. Zehrfeld and B.J. Green, Nucl. Fusion 12, 569 (1972).
- ⁷ E.K. Maschke and H.J. Perrin, Phys. Letters 102A, 106 (1984).

Figure Captions

Fig. 1: Fit of the experimental PDX results by a static equilibrium solution ($\underline{v} = 0$).

- (a) Temperature profile T/T_0
- (b) Mass density profile ρ/ρ_0

Fig. 2: Fit of the experimental PDX results by a toroidal flow equilibrium ($v_{\phi 0}/c_{s0} = 0.94$, $v_p = 0$)

- (a) Temperature profile T/T_0
- (b) Mass density profile ρ/ρ_0
- (c) Toroidal velocity v_{ϕ}/c_{s0}

Fig. 3: Fit of the experimental PDX results by a stationary equilibrium solution with very small net toroidal flow

- (a) Temperature profile T/T_0
- (b) Mass density profile ρ/ρ_0
- (c) Toroidal velocity v_{ϕ}/c_{s0}
- (d) Poloidal velocity v_p/c_{s0}

Fig. 4: Fit of the experimental PDX results by a stationary equilibrium solution with small toroidal flow located on the outside of the torus

- (a) Temperature profile T/T_0
- (b) Mass density profile ρ/ρ_0
- (c) Toroidal velocity v_{ϕ}/c_{s0}
- (d) Poloidal velocity v_p/c_{s0}

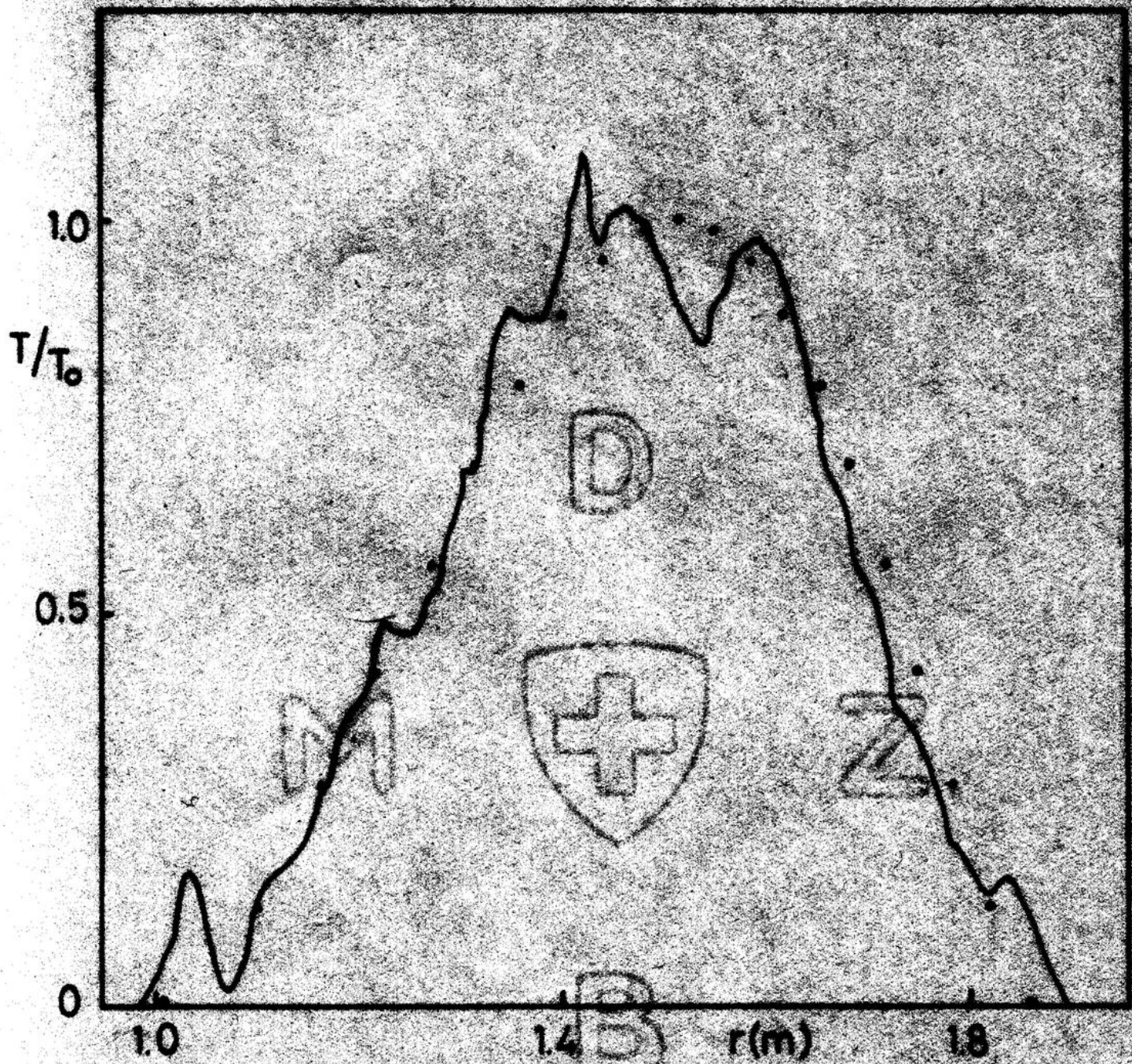
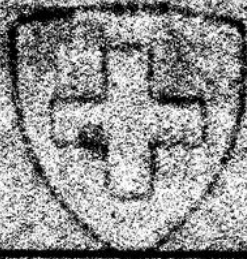


FIG. 1A

M



Z

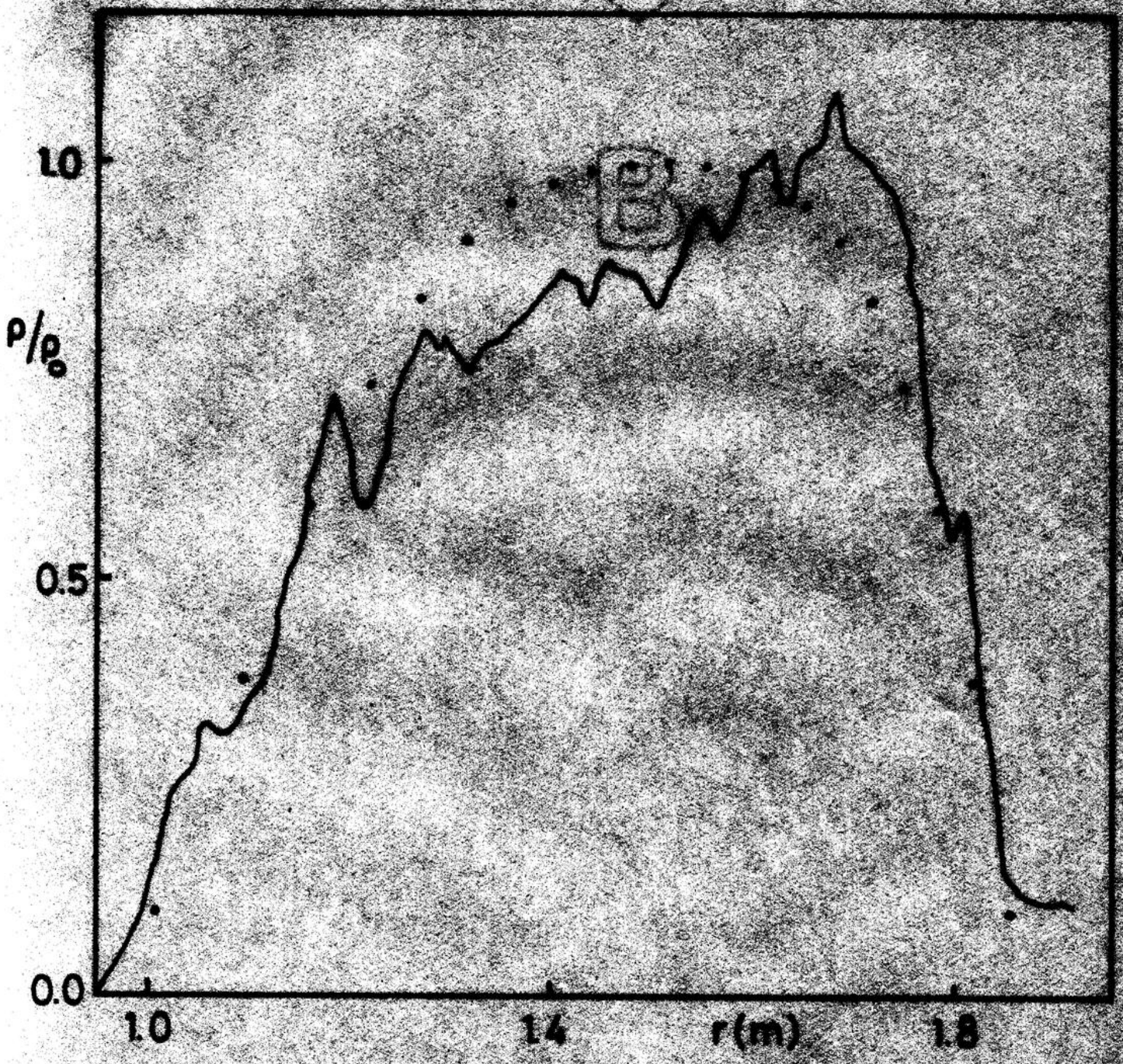
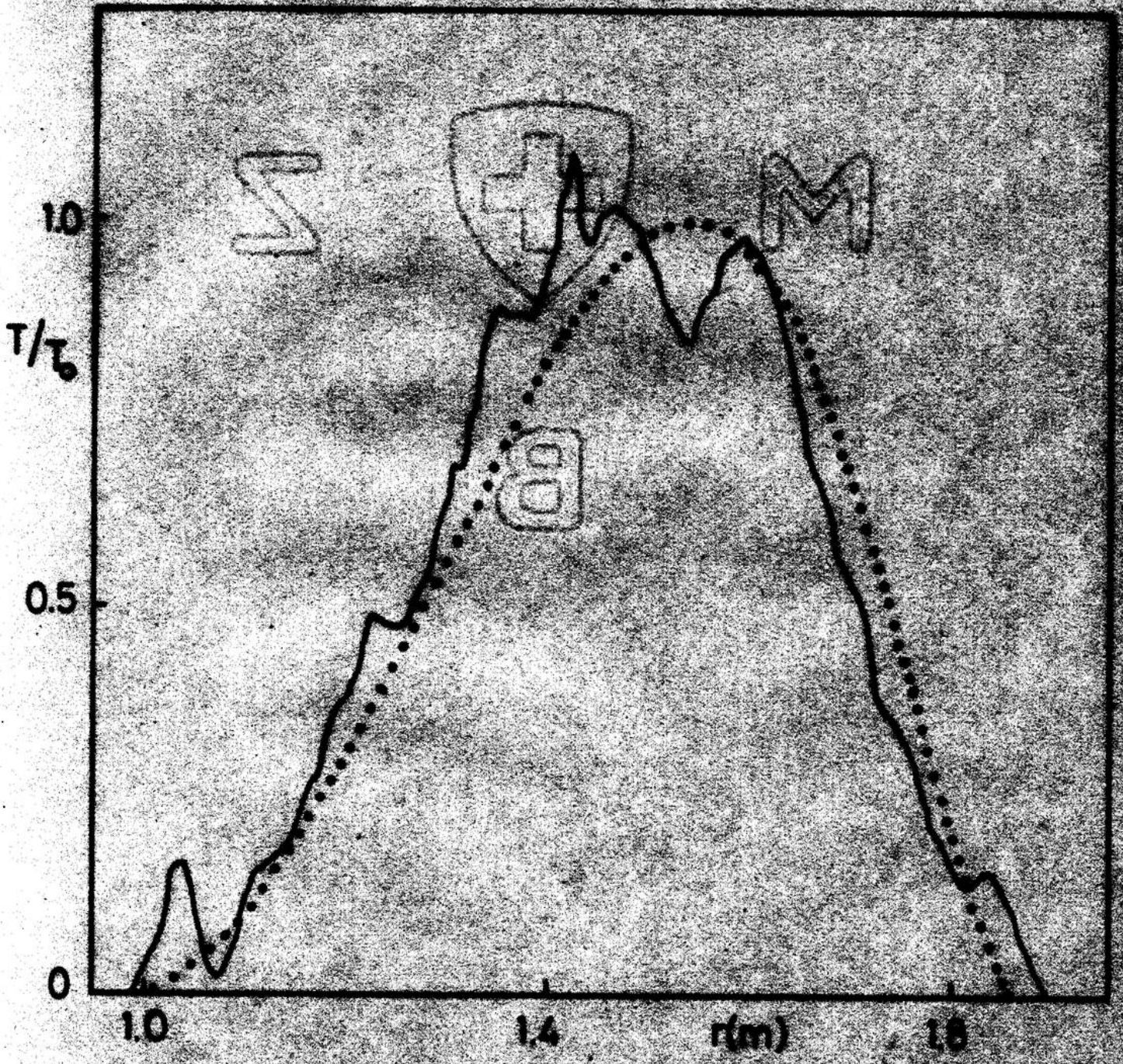
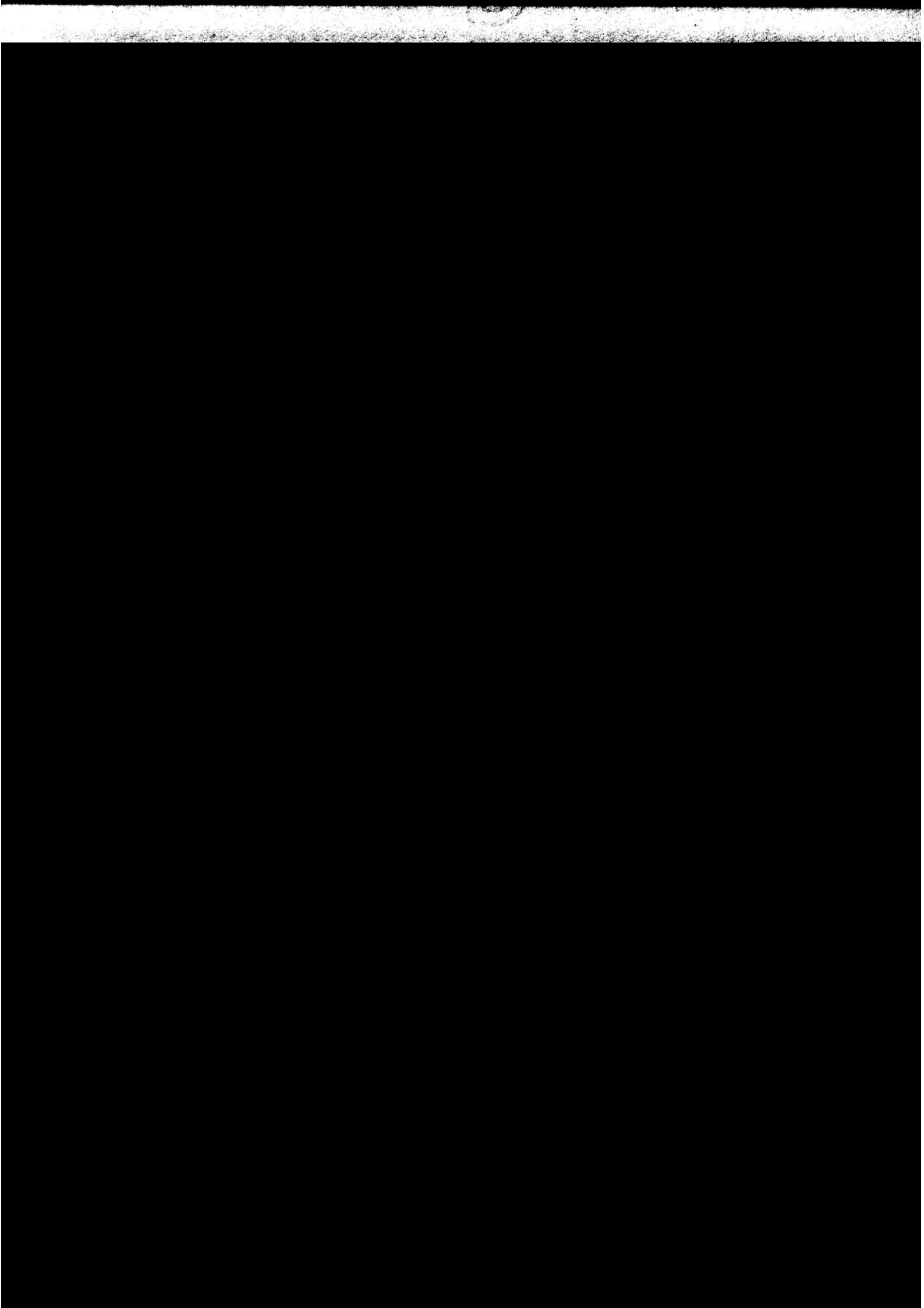


FIG. 1B

D







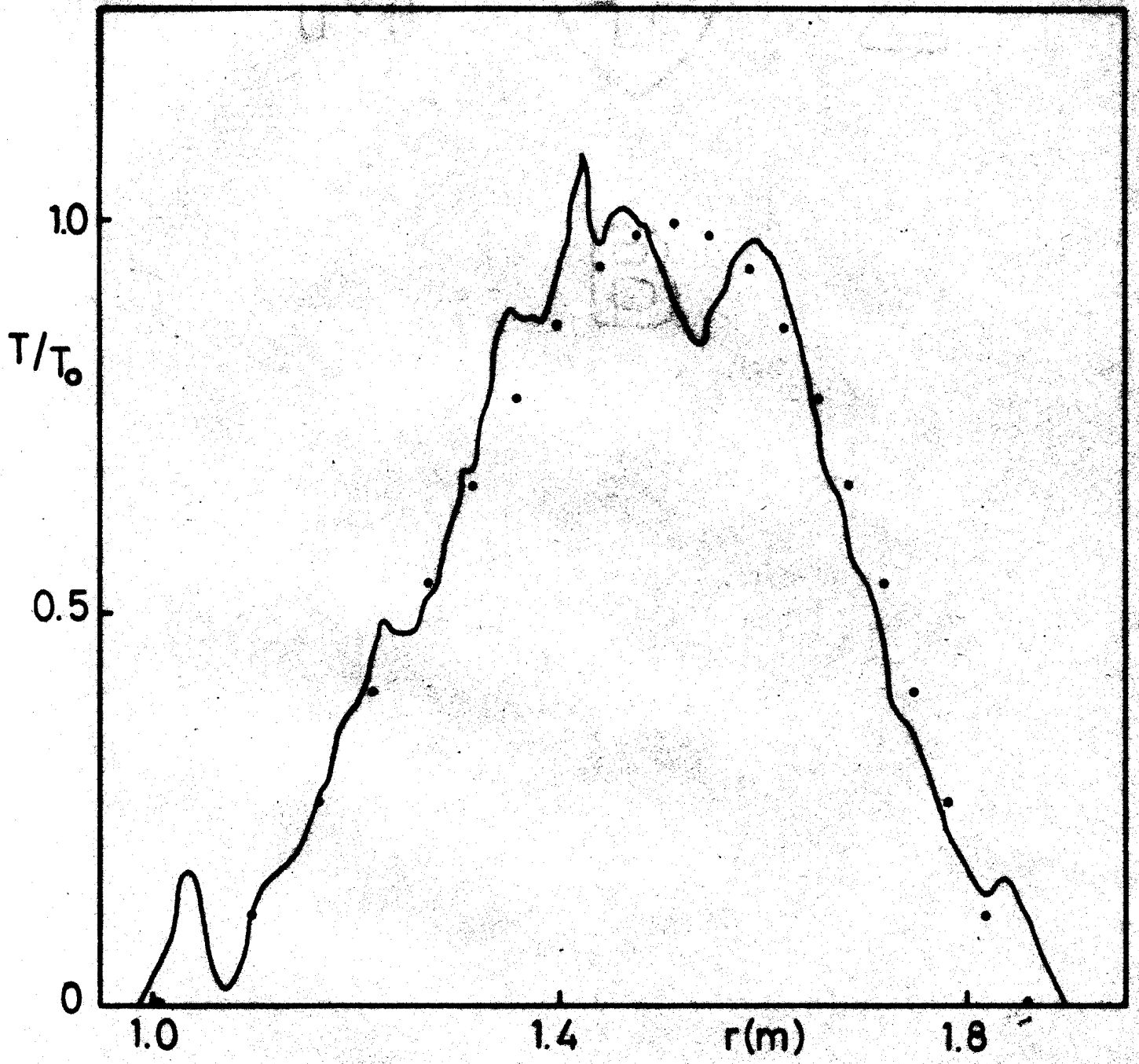
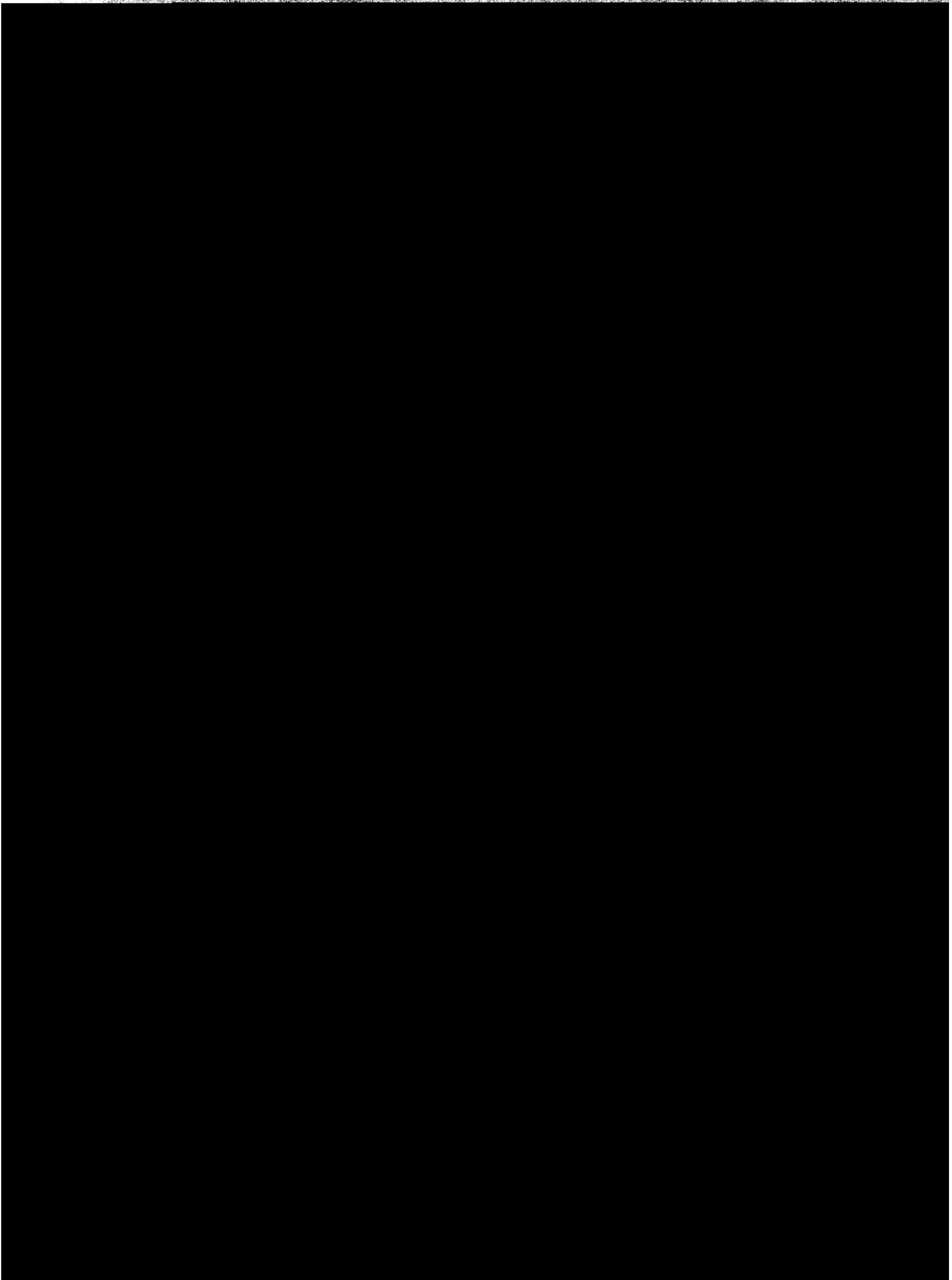
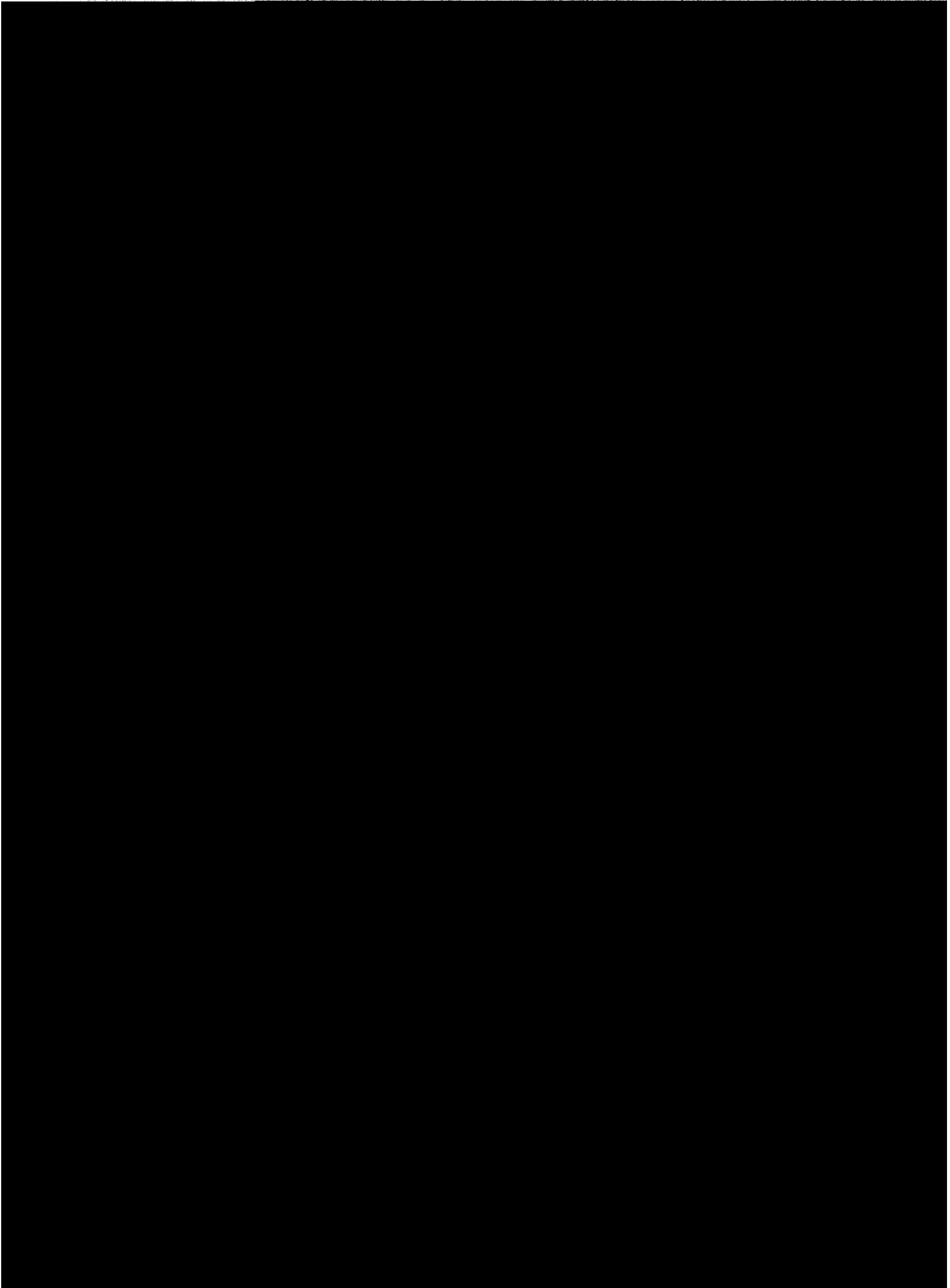
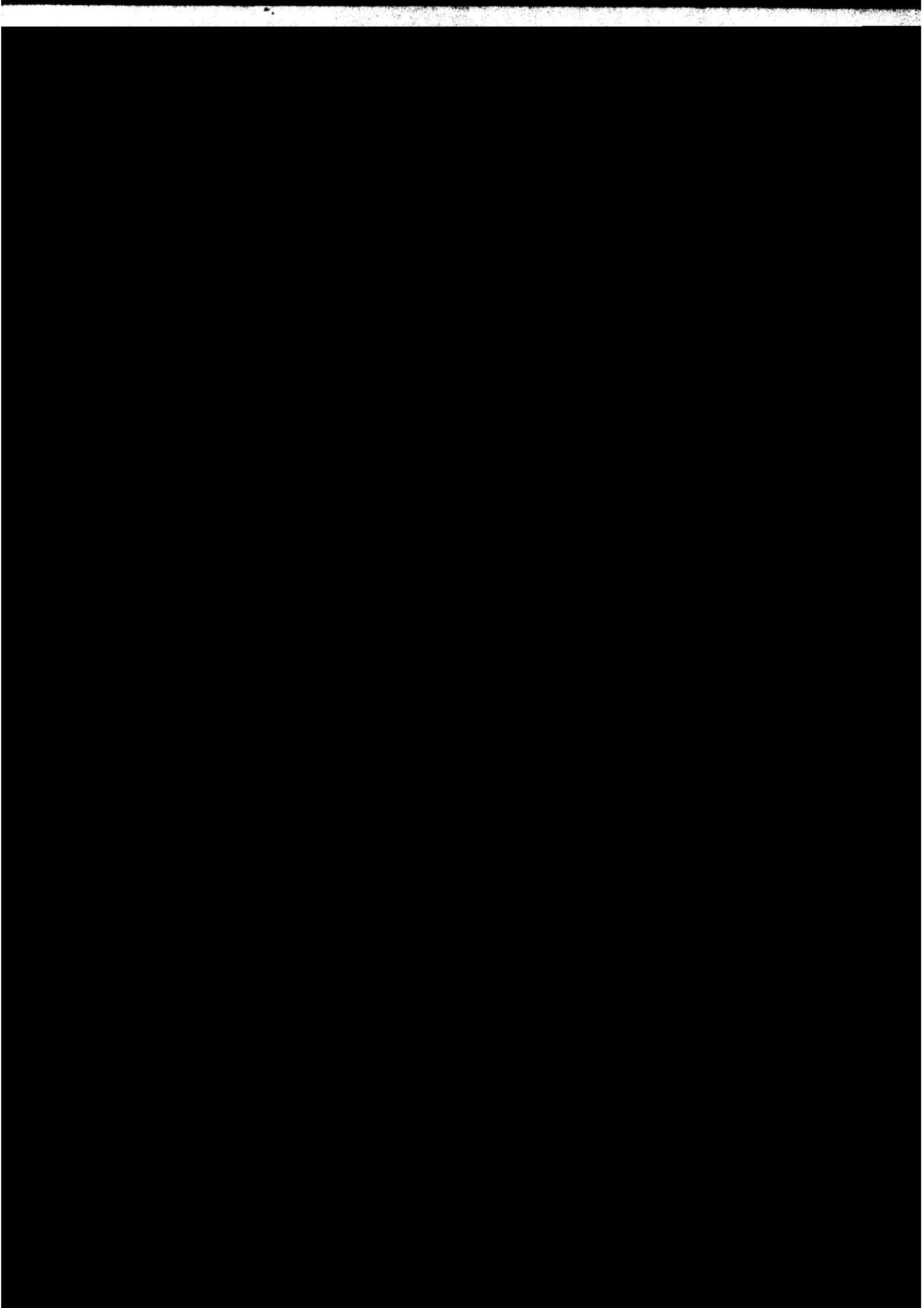


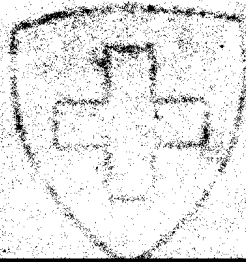
FIG. 3A







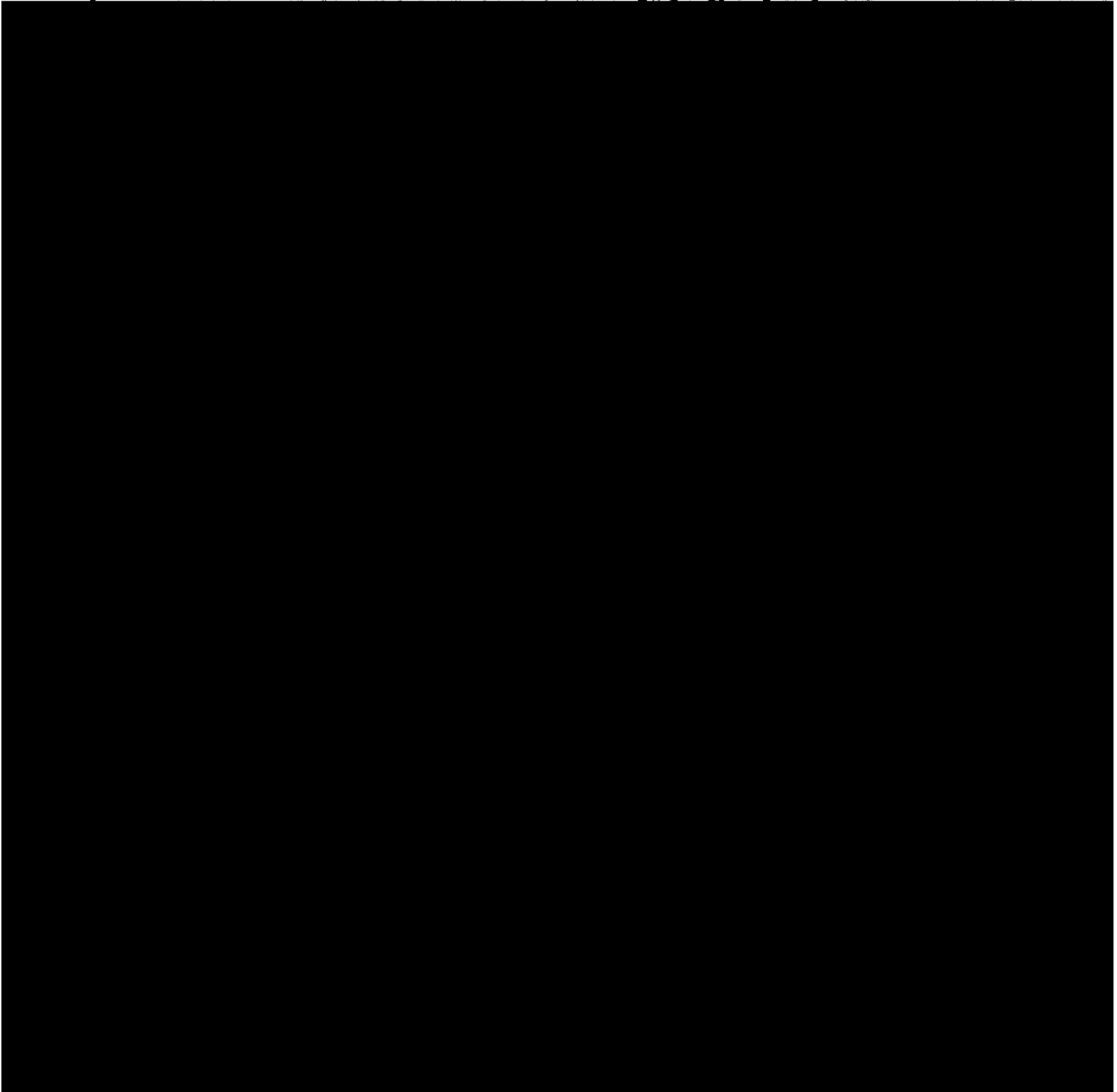
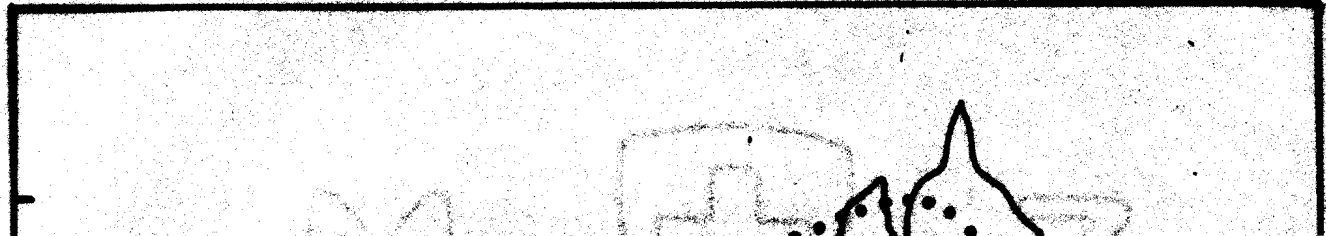
S

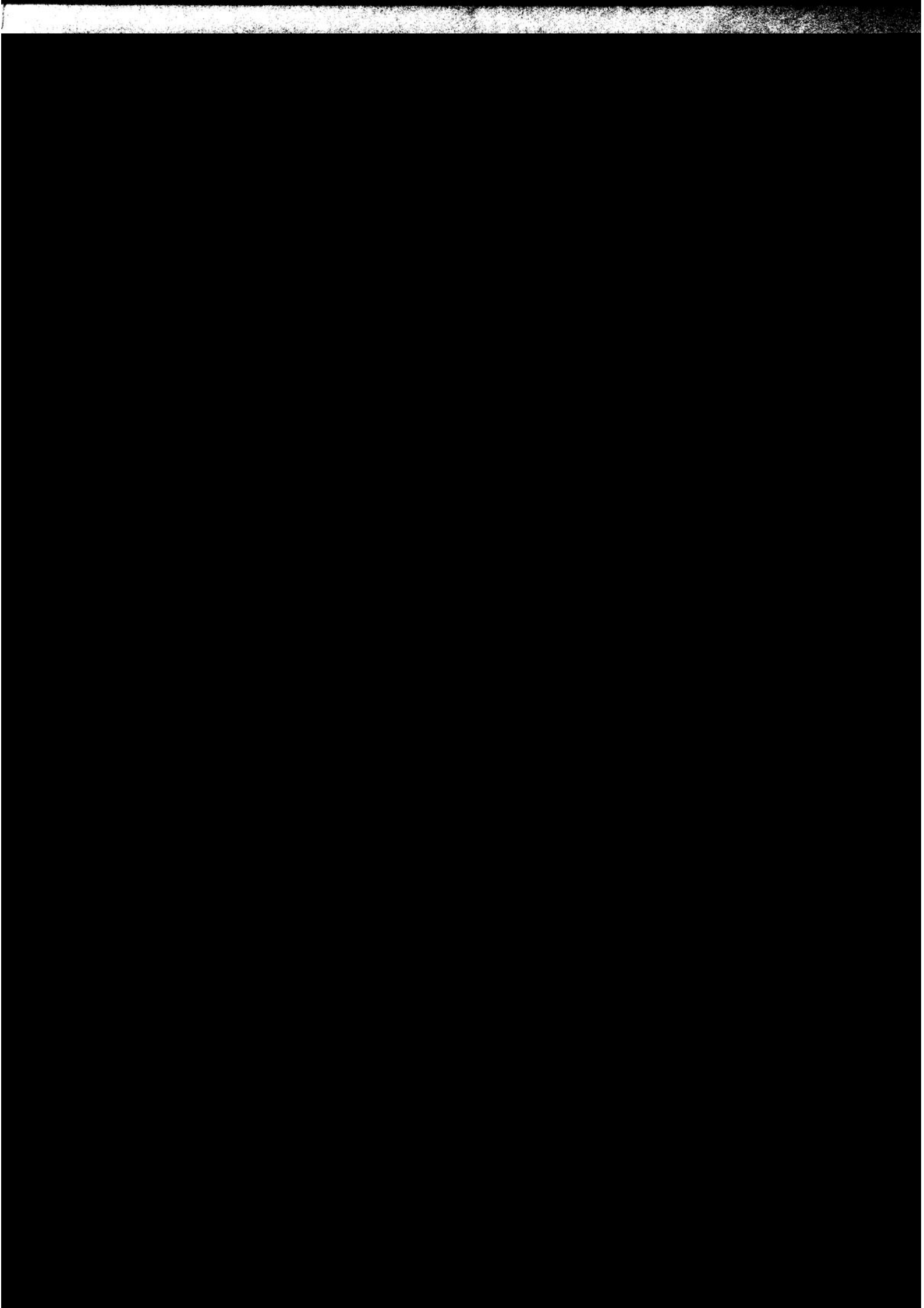


M

D

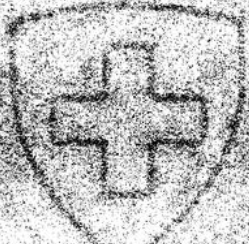
1.0





D

Σ



M

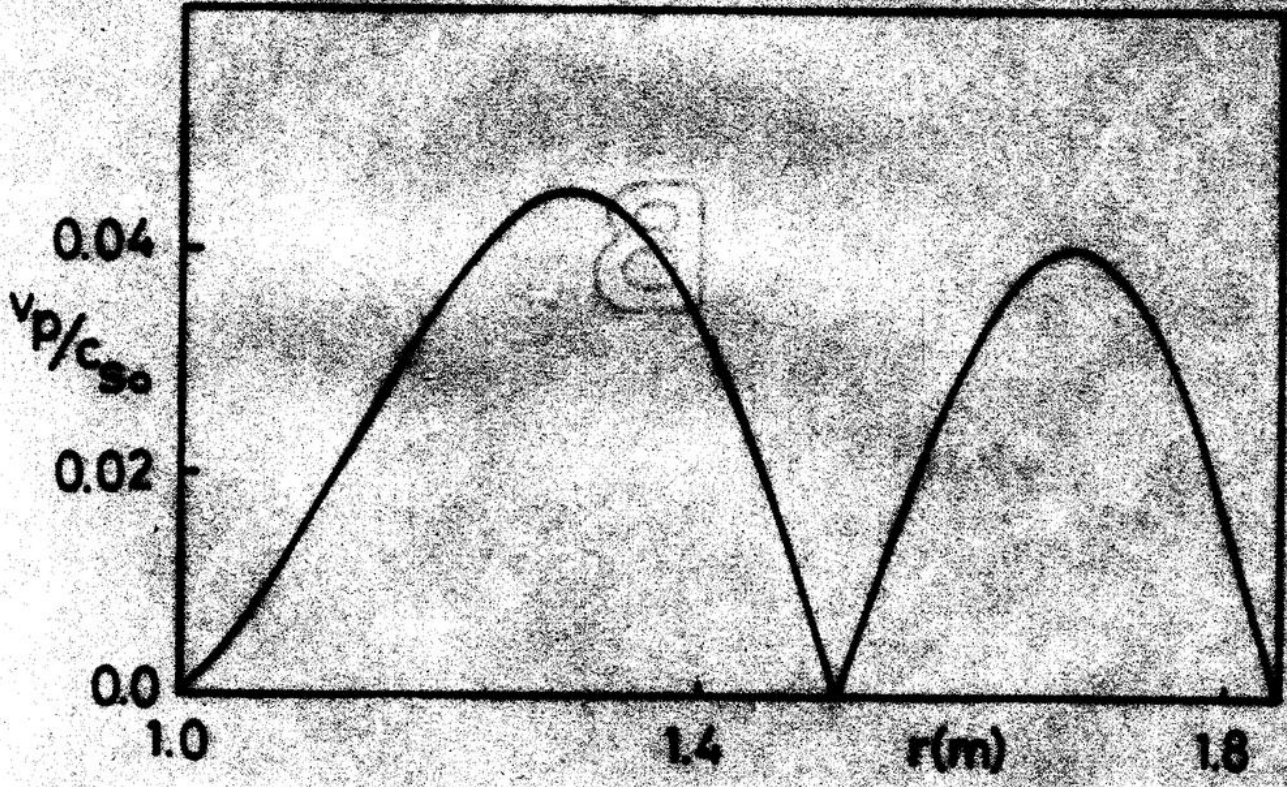


FIG. 4D